*Am J Physiol Gastrointest Liver Physiol* 303: G1254–G1261, 2012.
First published October 11, 2012; doi:10.1152/ajpgi.00107.2012.

# Loss of HGF activator inhibits foveolar hyperplasia induced by oxyntic atrophy without altering gastrin levels

**Yukinori Yamagata (山形幸徳),[1] Susumu Aikou (愛甲丞),[1] Tsuyoshi Fukushima (福嶋剛),[2] Hiroaki Kataoka (片岡寛章),[2] Yasuyuki Seto (瀬戸泰之),[1] Hiroyasu Esumi (江角浩安),[3] Michio Kaminishi (上西紀夫),[4] James R. Goldenring,[5] and Sachiyo Nomura (野村幸世)[1]**

[1]*Department of Gastrointestinal Surgery, Graduate School of Medicine, University of Tokyo, Tokyo, Japan;* [2]*Department of Pathology, Faculty of Medicine, University of Miyazaki, Miyazaki, Japan;* [3]*Research Center for Innovative Oncology, National Cancer Center Hospital East, Kashiwa, Japan;* [4]*Showa General Hospital, Kodaira, Japan; and* [5]*Nashville Veterans Affairs Medical Center and the Departments of Surgery and Cell and Developmental Biology, Epithelial Biology Center, Vanderbilt University School of Medicine, Nashville, Tennessee*

Submitted 15 March 2012; accepted in final form 8 October 2012

**Yamagata Y, Aikou S, Fukushima T, Kataoka H, Seto Y, Esumi H, Kaminishi M, Goldenring JR, Nomura S.** Loss of HGF activator inhibits foveolar hyperplasia induced by oxyntic atrophy without altering gastrin levels. *Am J Physiol Gastrointest Liver Physiol* 303: G1254–G1261, 2012. First published October 11, 2012; doi:10.1152/ajpgi.00107.2012.—Spasmolytic polypeptide/trefoil family factor 2 expressing metaplasia (SPEM) is induced by oxyntic atrophy and is known as a precancerous or paracancerous lesion. We now have sought to determine whether hepatocyte growth factor (HGF) influences the development of SPEM and oxyntic atrophy. DMP-777, a parietal cell ablating reagent, was administered to HGF activator (HGFA)-deficient mice and wild-type mice. Gastric mucosal lineage changes were analyzed in the DMP-777 treatment phase and recovery phase. Both wild-type and HGFA knockout mice showed SPEM, and there was no difference in SPEM development. However, after cessation of DMP-777, HGFA-deficient mice showed delayed recovery from SPEM compared with wild-type mice. Foveolar cell hyperplasia and the increase in proliferating cells after parietal cell loss were reduced in HGFA-deficient mice. The HGFA does not affect emergence of SPEM. However, the absence of HGFA signaling causes a delay in the recovery from SPEM to normal glandular composition. HGFA also promotes foveolar cell hyperplasia and mucosal cell proliferation in acute oxyntic injury.

metaplasia; gastric cancer; TFF2; HGF; SPEM

GASTRIC CANCER ARISES IN THE setting of atrophic gastritis caused by infection of *Helicobacter pylori* (*H. pylori*) (1, 23, 28). In the atrophic mucosa of the fundic glands of the stomach, spasmolytic polypeptide [trefoil family factor 2 (TFF2)] expressing metaplasia (SPEM), parietal cell loss, foveolar hyperplasia, as well as intestinal metaplasia, are observed. SPEM is associated with gastric cancer in the fundus at a higher rate than intestinal metaplasia and has been implicated as a precancerous lesion (4, 25, 29). The factors that can induce SPEM have not yet been identified, but several animal models produce SPEM, including mouse and rat *H. felis*/*H. pylori* infection models and administration of DMP-777 to mice and rats (3, 3a, 18, 19). DMP-777 is a cell-permeant neutrophil elastase inhibitor, which also acts as a parietal cell-specific protonophore and specifically ablates parietal cells. Treatment of mice with DMP-777 causes acute oxyntic atrophy, as well as foveolar hyperplasia, followed by the emergence of SPEM. Cessation of DMP-777 after administrating DMP-777 for 14 days leads to recovery of parietal cells, usually to a level greater than in untreated animals, and SPEM and foveolar hyperplasia resolve (19). In gastrin-deficient mice, compared with wild-type mice, SPEM appears earlier in response to DMP-777 administration and remains later after termination of drug treatment (19), even though hypergastrinemia accompanies atrophic gastritis in wild-type mice (9, 17).

Recent investigations have increasingly suggested that hepatocyte growth factor (HGF) plays an important role in the ontogeny and restoration of the gastrointestinal epithelium (8, 27). C-Met, which is the receptor for HGF, is overexpressed in gastric cancer, and HGF is implicated in gastric carcinogenesis. HGF was discovered in 1984 as the bioactive substance, which promoted the production and the expansion of hepatocytes (14). HGF was also identified as "scatter factor" (26), which controls scattering of kidney cells. HGF is secreted as an inactive single-chain form by mesenchymal cells and, following limited degradation by a serine protease, is converted into its activated two-chain form (15). Activated HGF acts as a mitogen, a motogen, and a morphagen for various cell lineages, including epithelial cells and inner skin cells through its receptor, c-Met tyrosine kinase (13, 14, 26). In the gastrointestinal mucosa, HGF is activated only in damaged lesions (11), and the efficiency of HGF activation is important for proliferation and restoration in the damaged mucosa.

HGF activator (HGFA), which resembles coagulation factor XII, is a serine protease, which is one of the most efficient activators of HGF. Other proteases, such as urokinase, tissue-type plasminogen activator, factor XII, factor XI, plasma kallikrein, matriptase, and hepsin can activate HGF in vitro. The latter two are transmembrane serine proteases, whereas the other five proteases originate from the plasma. All of these proteases are very weak activators of HGF, compared with HGFA, in vitro (12). HGFA is produced in the liver as an inactive protein form that is abundantly secreted into the circulation. In damaged organs, HGFA is activated by activated thrombin, degraded by kallikrein, and becomes a 34-kDa two-chain form (8). In the early stages of mucosal injury, HGFA is activated in damaged mucosa and promotes activation of HGF, which participates in mucous membrane restoration. Mucosal repair is impaired in the HGFA-deficient mouse, as HGF activation in the damaged legion is reduced by the lack of HGFA (7).

Address for reprint requests and other correspondence: S. Nomura, Dept. of Gastrointestinal Surgery, Graduate School of Medicine, Univ. of Tokyo, 7-3-1 Hongo, Bunkyo-ku, Tokyo 113-8655, Japan (e-mail: snomura-gi@umin.ac.jp).

The purpose of this study was to examine the participation of HGF in the generation of SPEM after loss of gastric parietal cells (acute oxyntic atrophy). Since HGF deficiency in mice is embryonic lethal, we employed the HGFA-deficient mouse model. We examined the changes in the gastric mucosal cell lineages of the HGFA-deficient mice when DMP-777 was administered compared with the changes in wild-type mice.

## MATERIALS AND METHODS

*Materials.* DMP-777, formulated at a concentration of 2% as a suspension in 0.5% methylcellulose, was a gift of DuPont Pharmaceuticals. 5-Bromo-2′-deoxyuridine (BrdU) was obtained from Sigma.

*Animals.* C57BL/6 mice were obtained from Charles River Breeding Laboratories. HGFA-deficient mice were made as previously described (7). During the experiments, mice were kept in cages provided with water and regular chow ad libitum until the time of death. All animal experimental procedures were reviewed and approved by the Institutional Animal Care and Research Advisory Committee of the University of Tokyo.

*Study design.* Male C57BL/6 wild-type control mice (8 wk of age) and male HGFA-deficient mice (8 wk of age) were administrated DMP-777 by oral gavage (350 mg/kg) once daily. Groups of six mice were killed before starting drug administration and after 1, 3, 7, 10, and 14 days of drug administration. Additionally, groups of three to eight mice, which received 14 days of drug administration, were killed 7 (R7), 14 (R14), and 28 (R28) days after cessation of 14-day drug administration.

*Necropsy and tissue processing.* BrdU in saline (200 mg/kg) was injected intraperitoneally in all mice 2 h before necropsy. Each mouse was anesthetized with avertin and was perfused through the left ventricle with PBS (pH 7.4) for 1 min, followed by 4% paraformaldehyde for 10 min. Each stomach was excised and opened along the greater curvature, then cut into 2-mm-wide strips parallel to the lesser curvature and embedded in paraffin. For histological studies, 5-μm sections were prepared.

For RNA extraction, the mice were killed by $CO_2$ inhalation, and the fundic regions of stomachs were excised, snap frozen with liquid nitrogen, and kept in −80°C until use.

*Histological examination.* We performed histochemistry and immunohistochemistry to explore the alterations in the gastric fundic mucosa. Histochemistry was performed for diastase-resistant periodic acid Schiff (DR-PAS) to detect surface mucous cells.

Murine monoclonal anti-H-K-ATPase IgG (a gift from Dr. Adam Smolka, Medical University of South Carolina, Charleston, SC), murine monoclonal anti-human TFF2 IgM (a gift from Dr. Nicholas Wright, Cancer UK, London, UK), and rabbit polyclonal anti-human intrinsic factor (IF) (a gift from Dr. David Alpers, Washington University, St. Louis, MO) were used as markers to identify parietal cells, mucous neck cells, and chief cells in fundic glands, respectively. For immunohistochemistry of anti-H-K-ATPase and anti-TFF2, deparaffinized sections were blocked using blocking serum provided in the HistoMouse staining kit (Zymed, South San Francisco, CA). Sections were incubated with a primary antibody (1:1,000 and 1:100 for anti-H-K-ATPase and anti-human TFF2, respectively) overnight at 4°C. Indirect immunohistochemical detection was then performed through incubation with biotinylated secondary antibodies and alkaline phosphatase-conjugated streptavidin (Vectastain ABC KIT, Vector Laboratories, Burlingame, CA). Chromogen was developed with Vector Red (Vector Laboratories).

For immunohistochemistry with anti-IF, deparaffinized sections were blocked with 1.5% normal goat serum and incubated with the primary antibody (1:1,000) overnight at 4°C, followed by incubation with a biotinylated second antibody and alkaline phosphatase-conjugated streptavidin. Chromogen was developed with Vector Red.

For immunohistochemistry of BrdU, a BrdU staining kit (Zymed) was used following the recommended instructions. In brief, sections were incubated in 0.25% trypsin for 2 min, followed by blocking of endogenous peroxidase activity with 3% $H_2O_2$. After incubation with a blocking serum, sections were incubated with biotinylated murine monoclonal anti-BrdU overnight at 4°C, followed by incubation with

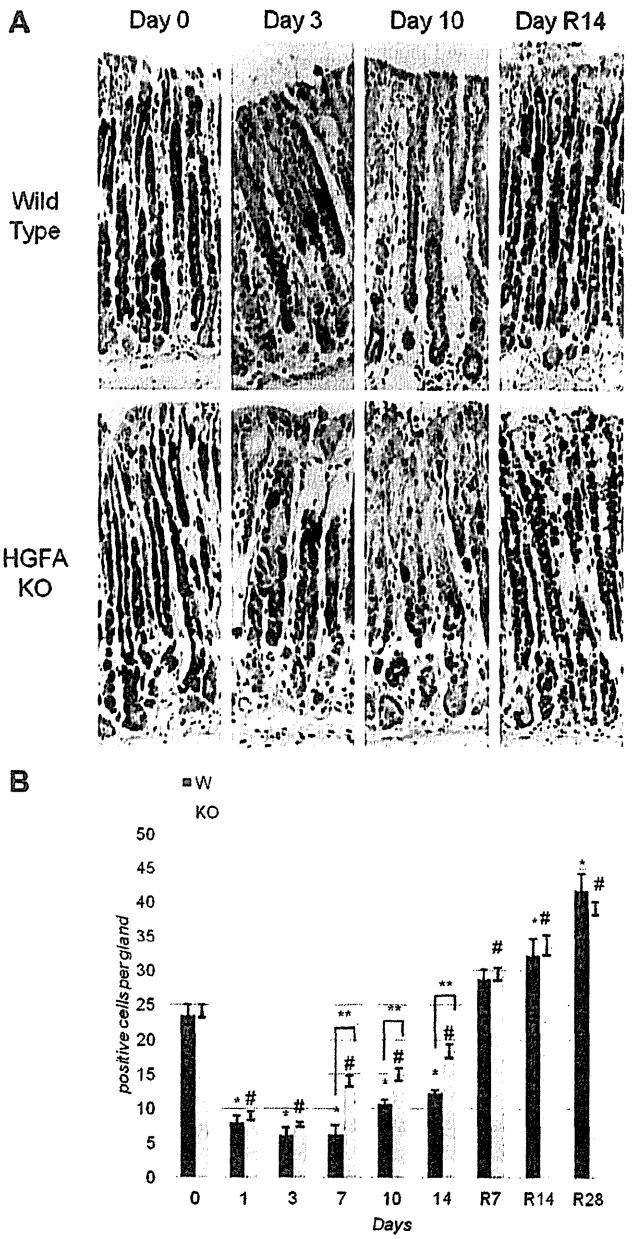


Fig. 1. Immunohistochemistry image for H-K-ATPase (*A*) and quantitation of the number of H-K-ATPase-positive cells per gland (*B*). Although both groups showed a significant reduction in the number of H-K-ATPase-positive cells at *day 3* of treatment, after recovery *day 7* (*day R7*), they recovered to the same level as untreated mice, and an overshoot was observed. Significant difference was observed on *days 7–14*. Numbers at each time point were compared with *day 0* by Dunnett's test. $*P < 0.05$ for wild-type (W) mice. $\#P < 0.05$ for knockout (KO) mice. Numbers for wild-type and KO mice at each time point were compared by Student's *t*-test. $**P < 0.05$. Values are means ± SE. HGFA, hepatocyte growth factor (HGF) activator.

horseradish peroxidase-conjugated streptavidin. Chromogen was developed with diaminobenzidine.

For immunostaining of activated c-Met, anti-phosphorylated (Y1235) human c-Met rabbit polyclonal antibody, which cross-reacts with mouse phosphorylated (Y1233) c-Met (6), was used. For immunostaining of HGF, rabbit polyclonal antibody raised against the amino-terminal amino acid sequence of HGF α-chain (IBL, Fujioka, Japan) was used. Immunohistochemical detection was performed according to the method described previously (6).

For all immunostaining, the sections were counterstained with Gill's hematoxylin and mounted.

*TUNEL method.* For analysis of HGF effect on apoptosis, the terminal deoxynucleotidyl transferase-mediated dUTP nick end labeling (TUNEL) method was applied. Apoalert DNA Fragmentation Assay Kit (Takara Bio, Otsu) was used according to the manufacturer's instructions.

*Quantitation of cell lineages.* Ten well-oriented glands were chosen from sections of the posterior wall of the fundic area of each stomach. The number of stained cells was determined, and the number of positive cells for each gland unit was calculated (visualized at ×200).

*RT-PCR for HGF.* Frozen fundic regions of the stomach were homogenized in ISOGEN-LS (Nippongene, Toyama), and total RNA was extracted according to the manufacturer's instructions. One microgram of total RNA was mixed with 0.25 μg of random primer (Promega, Tokyo) and incubated at 70°C for 10 min. Then first-strand buffer, dNTP mix, DTT, and Powerscript RT (Clontech, Otsu) were added and incubated at 42°C for 90 min. The reaction was terminated by heating at 70°C for 15 min.

Quantitative PCR was performed with an Eco real-time PCR system (Illumina, Tokyo), using MESA GREEN qPCR master mix plus for SYBR (EUROGENTEC, Toyama) as in the manufacturer's instructions. The PCR was performed with 40 cycles of 95°C for 1

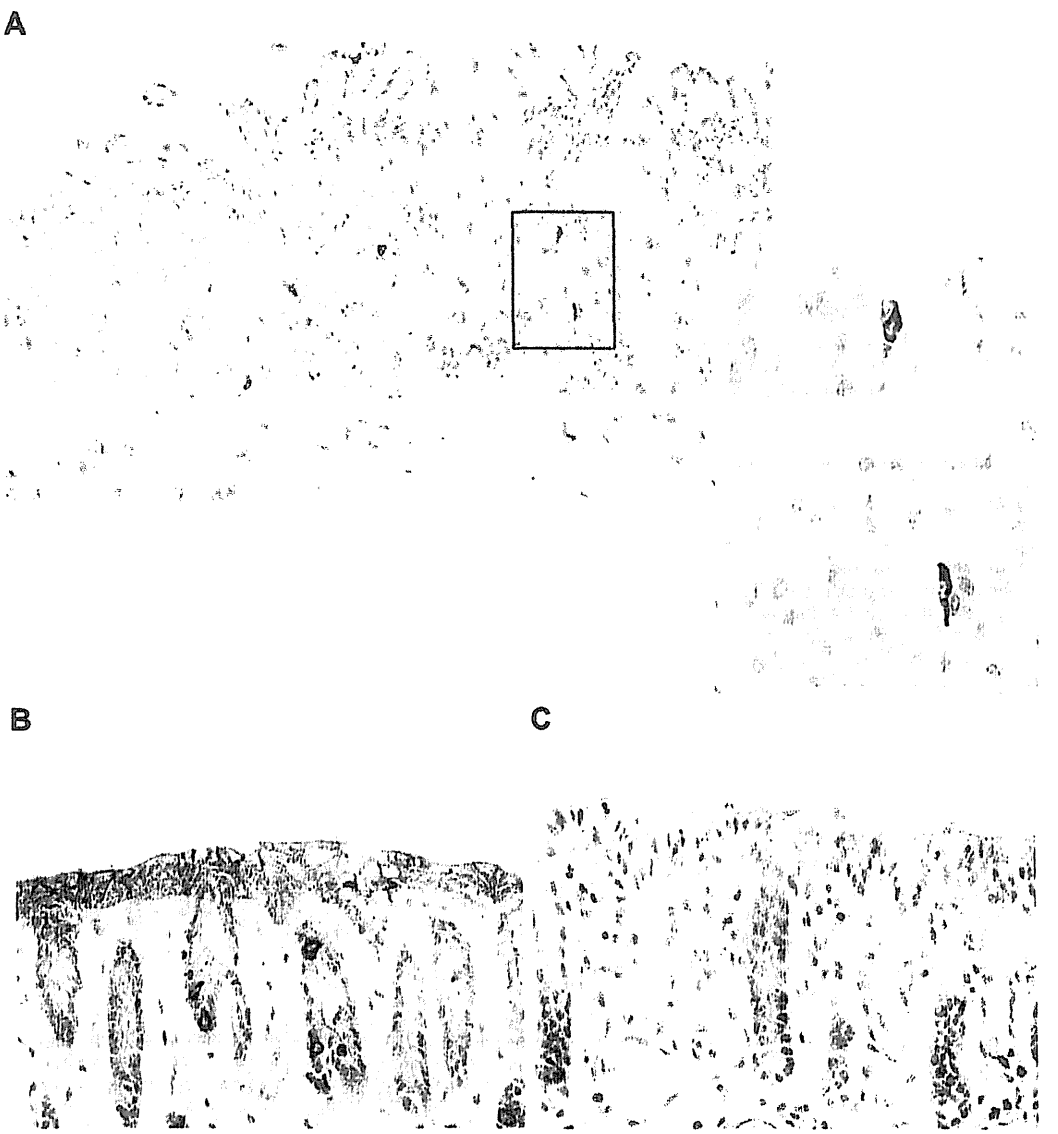


Fig. 2. Immunohistochemical staining for HGF (*A*) and activated c-Met (*B* and *C*). HGF was localized to scattered periglandular cells close to the middle of the glands. Activated c-Met was strongly positive in plasma membranes of foveolar cells in wild-type mice (*B*); however, only weak staining was present in HGFA KO mice (*C*). Some strongly stained cells were observed in the neck region of fundic glands of wild-type mice. The identity of these cells is unknown.

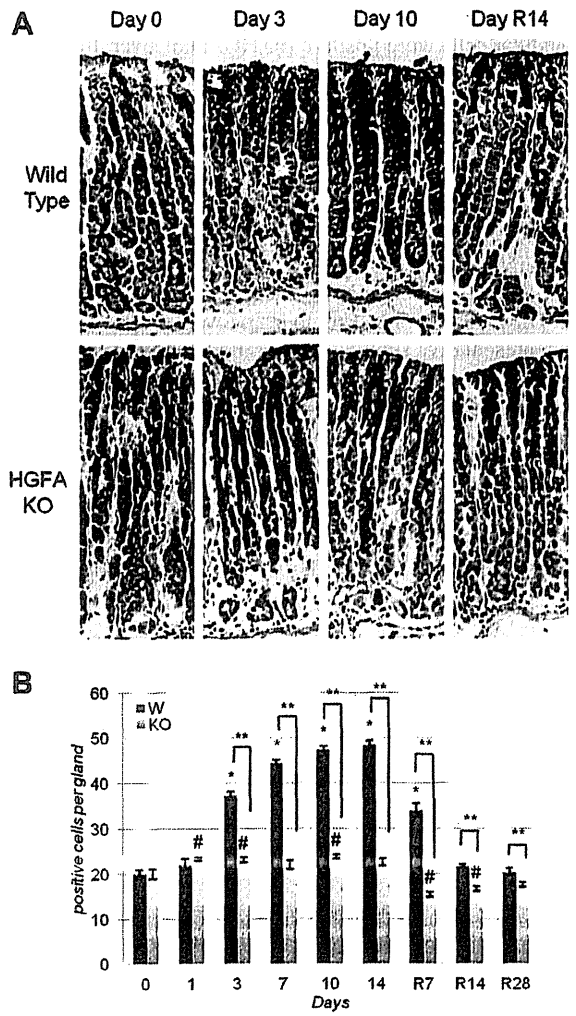


Fig. 3. Histochemistry for diastase-resistant periodic acid Schiff (DR-PAS) staining (*A*) and the quantitated changes in the number of DR-PAS-positive cells per gland (*B*). Although a remarkable increase in the number of DR-PAS-positive cells was observed after *day 3* in wild-type mice, these changes were not observed in HGFA KO mice. Foveolar cell numbers recovered to the untreated level in wild-type mice and were lower than original level in KO mice after *day R7*. After *day 3*, the number of DR-PAS-positive cells was significantly lower in KO mice compared with wild type. Numbers at each time point were compared with *day 0* by Dunnett's test. $*P < 0.05$ for wild type. $\#P < 0.05$ for KO mice. Numbers in wild-type and KO mice at each time point were compared by Student's *t*-test. $**P < 0.05$. Values are means ± SE.

min, 60°C for 30 s, and 72°C for 20 s. The forward primer for the control GAPDH was CGTCCCGTAGACAAAATGGT, the reverse primer for GAPDH was AATTTGCCGTGAGTGGAGTC, the forward primer for HGF was TTCCCAGCTGGTCTATGGTC and the reverse primer for HGF was TGGTGCTGACTGCATTTCTC.

*Measurement of serum gastrin levels.* Blood gathered from the right atrium of the mouse was centrifuged at 3,000 rpm for 10 min, and the supernatant was collected and saved at −80°C until use. The serum gastrin levels were measured by radioimmunoassay by SRL (Tachikawa, Tokyo).

*Statistical analysis.* All statistical analyses were performed using JMP7 software. The number of cells and the serum gastrin levels were evaluated by ANOVA, Dunnett test, and Student's *t*-test. Dunnett test was used for comparison of the value of each time point to the value of *day 0* in each mouse group. Student's *t*-test was performed when the values of wild-type and HGFA knockout (KO) mice were compared at each time point. *P* values $< 0.05$ were considered statistically significant.

## RESULTS

*Parietal cell loss induced by DMP-777.* The cells immunoreactive for the α-subunit of H-K-ATPase were counted as parietal cells. Figure 1*A* shows representative pictures of immunostaining for H-K-ATPase, and Fig. 1*B* shows the number of H-K-ATPase-positive cells per gland. One day after DMP-777 administration, the number of H-K-ATPase-positive cells decreased to 33–37% of untreated mice in both wild-type and HGFA-deficient mice, and, after 3 days of treatment, the number decreased to 26–32%. The number of parietal cells was reduced throughout DMP-777 treatment. However, as previously reported,

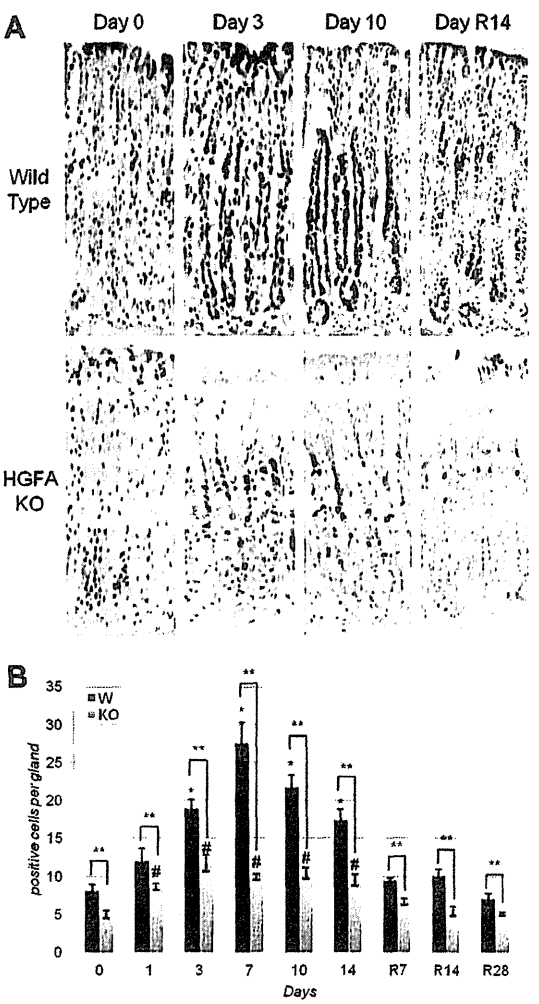


Fig. 4. Immunohistochemical staining for 5-bromo-2′-deoxyuridine (BrdU; *A*) and quantitation of the number of BrdU-positive cells per gland (*B*). In both groups, the number of BrdU-positive cells significantly increased after *day 3* and returned to the untreated level by *day R7*. The number of BrdU-positive cells was significantly lower in KO mice than in wild-type mice at all time points. Numbers at each time point were compared with *day 0* by Dunnett's test. $*P < 0.05$ for wild type. $\#P < 0.05$ for KO. Numbers in wild-type and KO mice at the same time point were compared by Student's *t*-test. $**P < 0.05$. Values are means ± SE.

after 7 days of treatment, we did observe some recovery of parietal cells. This recovery was complete and reached levels greater than in untreated mice after R7 and R14 days off of drug treatment. An increase of 23–78% was observed at *days R7*, *R14*, and *R28* compared with the level before administration. The number of H-K-ATPase-positive cells in the HGFA KO group was significantly greater than that of wild-type group 7–14 days after beginning the DMP-777 administration, but, in the recovery phase after withdrawal of DMP-777 treatment, recovery of H-K-ATPase-positive cells was equivalent. The number of H-K-ATPase-positive cells after DMP-777 administration in both groups increased with time of recovery, with R7 < R14 < R28. The overshoot of parietal cell numbers was maintained at least until R28 in both groups.

*HGF activation after acute parietal cell loss.* To confirm that the origin of HGF is not parietal cells, we examined the immunolocalization of HGF and quantitative RT-PCR for HGF before and after administration of DMP-777. By quantitative RT-PCR, in wild-type mice there was no difference in HGF mRNA expression in the fundic mucosa comparing untreated mice and mice treated with DMP-777 for 10 days (data not shown). HGF immunostaining is shown in Fig. 2*A*. Several periglandular cells were positive for HGF; however, there was no detectable staining in parietal cells.

To assess the HGF activation in wild-type mice and HGFA KO mice, activated c-Met immunostaining was performed. As shown in Fig. 2*B*, activated c-Met was strongly positive in cell membranes of foveolar cells and in some cells in the neck region, but only in wild-type mice (Fig. 2*C*). Foveolar cell membranes of HGFA KO mice demonstrated only weak staining for activated c-Met.

*Foveolar cell numbers after acute parietal cell loss.* We utilized DR-PAS histochemistry to stain foveolar cells. Figure 3*A* shows representative staining for DR-PAS, and Fig. 3*B* shows the changes in the number of foveolar cells per gland. In untreated mice, the number of DR-PAS-positive cells in wild-type and HGFA-deficient mice was equivalent. A significant foveolar cell hyperplasia was observed only in wild-type mice. After 3 days of DMP-777 administration and after 14 days of treatment, the number of DR-PAS-positive cells increased 2.4-fold over the numbers in untreated mice. On the other hand, in HGFA KO mice, although there was a statistically

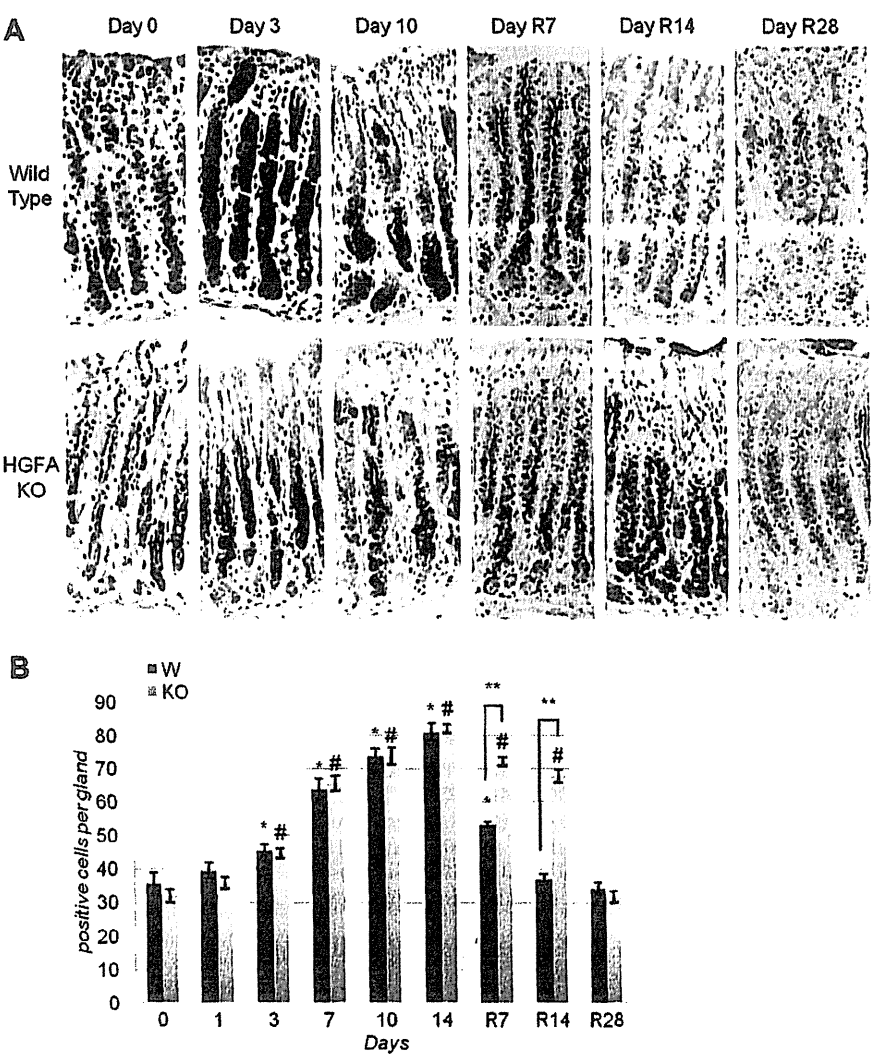


Fig. 5. Immunohistochemical staining for trefoil family factor 2 (TFF2; *A*) and the quantitation of the changes in the numbers of TFF2-positive cells per gland (*B*). Numbers of TFF2-positive cells in wild type and KO are similar on *days 0–14*. In KO mice, the number of TFF2-positive cells was significantly higher compared with wild type at *days R7* and *R14*. Recovery from spasmolytic polypeptide/TFF2 expressing metaplasia to normal glands was slower in KO mice. Numbers at each time point were compared with *day 0* by Dunnett's test. $*P < 0.05$ for wild type. $\#P < 0.05$ for KO mice. Numbers of wild-type and KO mice were compared at each same time point by Student's *t*-test. $**P < 0.05$. Values are means ± SE.

significant increase in foveolar cells compared with *day 0*, the increase was much reduced (10–18%) compared with the changes in wild-type mice. By *day R14*, the number of DR-PAS-positive cells returned to its initial level in wild-type mice and showed a small decrease in HGFA KO mice. Comparing both groups, the number of foveolar cells in HGFA KO mice was significantly smaller than that in wild-type mice, from *day 3* of DMP-777 treatment through *day R28*.

*Effects of acute parietal loss on S-phase proliferating cells.* BrdU staining was used to assess S-phase proliferating cell lineages. Figure 4*A* shows representative immunohistochemistry images of BrdU staining, and Fig. 4*B* displays the changes in the number of BrdU-positive cells per gland. Both groups showed increased numbers of proliferating cells beginning 1 day after DMP-777 administration. The increases in proliferation peaked at 2.0- to 3.4-fold at *day 7* and then declined afterwards. Proliferation in both groups returned to the untreated levels by *day R7*. HGFA KO mouse stomachs showed significantly fewer BrdU-positive cells throughout the whole period compared with wild-type mice.

*Alterations in TFF2-positive cells and induction of SPEM in response to parietal cell loss.* Figure 5*A* shows representative figures of immunohistochemical staining of TFF2, and Fig. 5*B* shows the changes in the numbers of TFF2-positive cells per gland. In the normal fundic glands in untreated mice, TFF2 stained in mucous neck cells, which are located in the middle third of the gland. Before DMP-777 administration, TFF2-positive cells resided around the middle of the gland in both wild-type and HGFA KO mice, and the number of TFF2-positive cell was equivalent in both types. The number of TFF2-positive cells began to increase significantly from *day 3* of DMP-777 administration and continued to rise until *day 14* of treatment, with appearance of SPEM expanding from the bases of glands. Although there was no difference between groups during DMP-777 administration, at *days R7* and *R14*, the number of TFF2-positive cells in HGFA KO mice remained significantly higher than in untreated mice, while the numbers TFF2-immunoreactive cells in wild-type mice returned to the level in untreated mice by *day R14*. In comparison between both groups, the number of TFF2-positive cells in HGFA KO was significantly higher than in wild-type mice at *days R7* and *R14*. These results indicate that the loss of SPEM following removal of DMP-777 in HGFA KO mice was delayed compared with that in wild-type mice. On *day R28*, the number of TFF2-positive cells returned to the same level as *day 0* in both groups of mice.

*Effects of oxyntic atrophy of expression of IF.* The immunohistochemical staining of IF was used as a maker of chief cells. Figure 6*A* shows representative figures of immunohistochemical staining of IF, and Fig. 6*B* shows the changes in the numbers of IF-positive cells per gland. We observed a small decrease in the number of IF-positive cells on *days 3–14* of treatment (wild-type 10–25% and HGFA KO 2–10% decrease), although neither change was statistically significant. In *days R7–R28* mice, the number of IF-positive cells recovered to the untreated levels in both groups.

*Effects of oxyntic atrophy on apoptosis.* Apoptosis was assessed by the TUNEL method. As shown in Fig. 7*A*, TUNEL-positive cells were localized to foveolar cells close to the mucosal surface. Apoptotic cell numbers were much higher in wild-type mice than in HGFA KO mice without treatment (Fig. 7*B*). After DMP-777 treatment, apoptotic cell numbers decreased significantly compared with untreated mice only in wild-type mice from *day 1* to *day R7*. No change in apoptotic cell numbers was observed in HGFA KO mice throughout the treatment period. On *days 0, R14*, and *R28*, the apoptotic cell number was significantly higher in wild-type mice compared with HGFA KO mice.

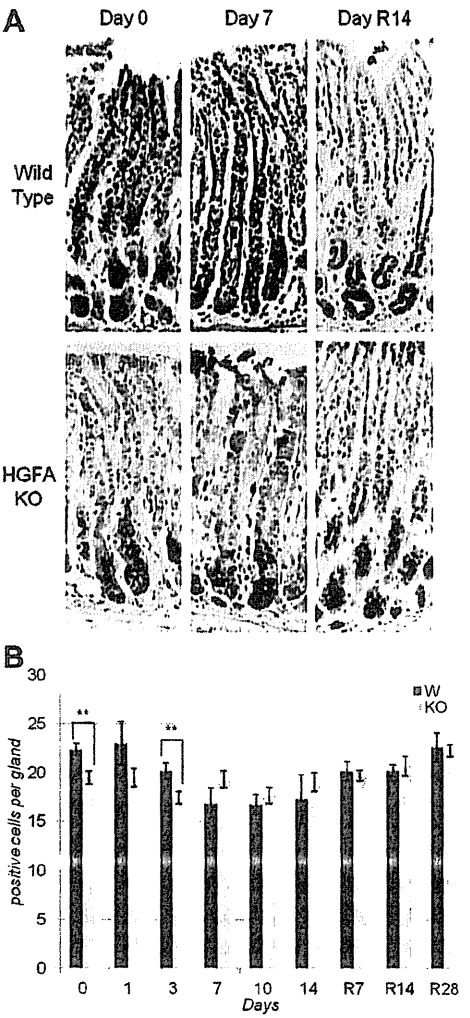


Fig. 6. Immunohistochemical staining for intrinsic factor (IF; *A*) and the quantitation of the changes in the numbers of IF-positive cells per gland (*B*). Although there was a tendency for decreasing numbers of IF-positive cells during DMP-777 treatment, there was no significant difference from the original number in either group. Numbers at each time point were compared with *day 0* by Dunnett's test. $^{**}P < 0.05$. Values are means ± SE.

*Serum gastrin levels after induction of oxyntic atrophy.* Our laboratory has previously reported that the hyperplasia of foveolar cells after DMP-777 treatment depended on an increase in gastrin, as exemplified by the absence of foveolar hyperplasia in gastrin-deficient mice treated with DMP-777 (10). Because the change in the number of foveolar cells was significantly different between wild-type and HGFA KO in these studies, we measured serum gastrin level.

Figure 8 shows the changes of serum gastrin levels. Both groups showed a significant rise of the serum gastrin level on *days 1–14* of DMP-777 treatment. The serum gastrin levels dropped on *day 14*, but were still elevated compared with the level on *day 0*.

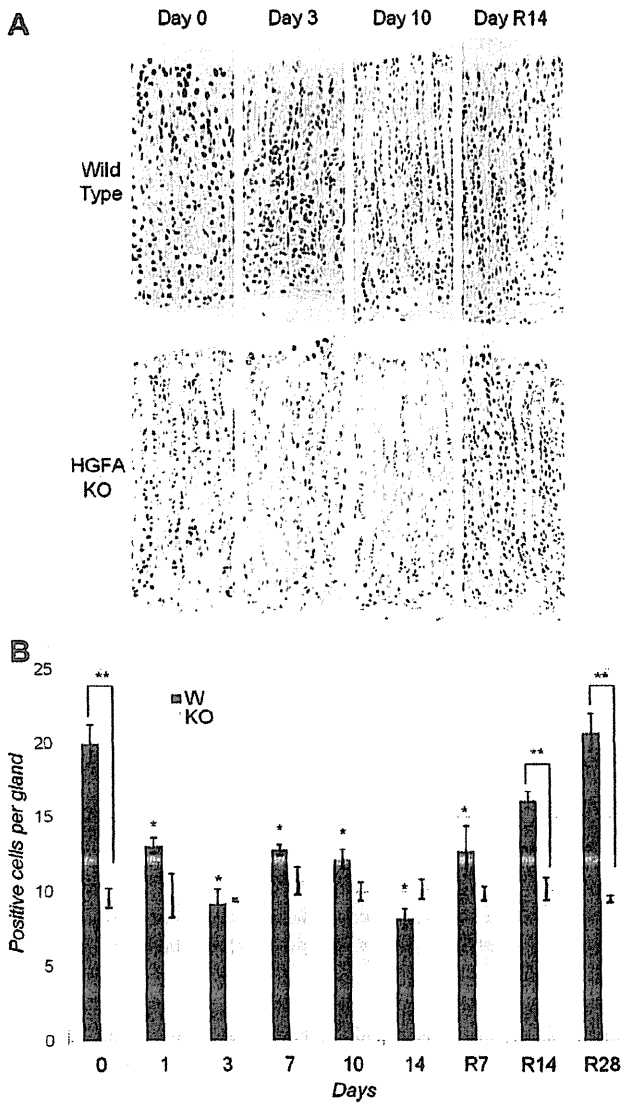


Fig. 7. Terminal deoxynucleotidyl transferase-mediated dUTP nick end labeling (TUNEL) staining in wild-type and HGFA KO mice (*A*) and quantitation of the numbers of apoptotic cells per gland (*B*). TUNEL-positive cells were localized to foveolar cells close to the surface of mucosa. The number of TUNEL-positive cells was much higher in wild-type mice compared with HGFA KO mice. DMP-777 administration caused a reduction in the number of TUNEL-positive cells to a level similar to that in HGFA KO mice. The number of TUNEL-positive cells was not changed by DMP-777 administration in HGFA KO mice. $*P < 0.05$ in wild type. $**P < 0.05$. Values are means ± SE.

## DISCUSSION

Gastric cancer arises in the setting of atrophic gastritis, which is accompanied by foveolar cell hyperplasia and SPEM formation. In this study, foveolar cell hyperplasia was observed in wild-type mice following DMP-777-induced parietal cell loss, but was not observed in HGFA-deficient mouse after induction of oxyntic atrophy. These findings suggest that HGF is needed for foveolar cell hyperplasia formation in atrophic gastritis. In support of this, activated c-Met was positive in the plasma membranes of foveolar cells only in wild-type mice and was absent in HGFA KO mice. HGF is activated in the gastric mucosa by activated HGFA when the mucosa is damaged, and foveolar hyperplasia is one of the defensive changes in the gastric mucosa (8, 13, 21, 22). Our laboratory has reported previously that foveolar cell hyperplasia was not observed in gastrin-deficient mouse following DMP-777 administration (19). In the present studies, the serum gastrin levels were elevated in HGFA-deficient mice after DMP-777 treatment to the same extent as seen in wild-type mice through 10 days of administration. Nevertheless, foveolar cell hyperplasia was essentially absent in DMP-777-treated HGFA-deficient mice. These results indicate that both HGF and gastrin are needed for induction of foveolar cell hyperplasia, and that induction of HGF activation must lie downstream of, or be permissive for, gastrin stimulation of foveolar cell production. In support of this concept, HGF is induced by the gastrin stimulation in cultured gastric cancer cells (10). How gastrin stimulation leads to HGF activation and foveolar cell hyperplasia remains to be determined in the future.

In untreated mice, the number of both BrdU-positive cells and apoptotic cells were higher in wild-type mice compared with HGFA KO mice. As there was no difference in the number of mucosal cell lineages in both mice, cell proliferation and apoptosis are balanced in HGFA KO mice by hypoproliferation and hypo-apoptosis. Although an increase in BrdU-positive cells was observed during the DMP-777 dosing period in both groups, we observed a smaller increase in HGFA-deficient mice compared with wild-type mice. Apoptotic cell number was dramatically reduced in wild-type mice during the DMP-777 dosing period, but no changes were found in HGFA KO mice. Foveolar hyperplasia can result from hyperproliferation in the neck of the fundic glands, as well as from reduction of apoptosis in foveolar cells in wild-type mice. Thus HGF likely promotes both cell proliferation and apoptosis in the normal gastric mucosa, and further increases cell proliferation without promoting apoptosis in the atrophic mucosa. In atrophic gastritis, HGF promote tumor growth and cell proliferation and anti-apoptosis.

Our laboratory has reported that "transdifferentiation" of chief cells, expressing IF, accounts for the origin of SPEM (2, 16, 20). In the normal fundic gland, mucous neck cells migrate toward the bottom of the gland and, at the same time, differentiate into the chief cell. In generating SPEM, our laboratory has reported that

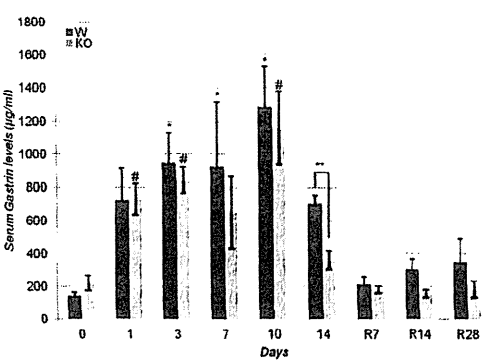


Fig. 8. Serum gastrin levels in wild-type and HGFA KO mice. Serum gastrin levels in both groups increased on *day 1* of DMP-777 treatment and remained elevated until *day 10*. On *day 14*, the level of both groups decreased. In comparisons between the groups, a significant difference was observed only on *day 14*. Numbers at each time point were compared with *day 0* by Dunnett's test. $*P < 0.05$ in wild type. $\#P < 0.05$ in KO. Numbers in wild-type and KO mice at the same time point are compared by Student's *t*-test. $**P < 0.05$. Values are means ± SE.

the mature chief cell transdifferentiates into TFF2-expressing SPEM cells in the setting of acute oxyntic atrophy (2, 16, 20). In this experiment, the emergence of SPEM and the change in the number of TFF2-positive cells were equivalent in both wild-type and HGFA-deficient mice, even though the increase of BrdU-positive cells was smaller in HGFA-deficient mice. This result supports the concept that the origin of SPEM following DMP-777 treatment is predominantly due to "transdifferentiation" rather than activation of a cryptic proliferative cell population.

The association of SPEM with gastric cancer in humans suggests that SPEM may be a precancerous lesion. Because it was reported that HGF contributed to the development of gastric cancer (5, 6), it seemed possible that SPEM formation would be promoted by HGF. However, no difference in SPEM formation following acute oxyntic atrophy was observed in HGFA-deficient mice, even though parietal cell numbers were slightly higher in HGFA-deficient mice from *day 7* through *day 14*. On the other hand, after the end of DMP-777 administration, a delay in the recovery from SPEM back to a normal mucosa was observed in HGFA-deficient mouse. Thus HGF and HGFA do appear to contribute to the recovery of the damaged mucosa from SPEM to normal lineages. These results support the concept that HGF and HGFA promote normal cell differentiation in the gastric fundic mucosa. Thus loss of HGFA prevents gastrin-stimulated foveolar hyperplasia and delays the normal recovery from oxyntic atrophy.

## ACKNOWLEDGMENTS

We thank Miki Furuya for technical assistance. We also thank Dr. Nicholas Wright, Dr. Adam Smolka, and Dr. David Alpers for kind gifts of antibodies.

## DISCLOSURES

No conflicts of interest, financial or otherwise, are declared by the author(s).

## AUTHOR CONTRIBUTIONS

Author contributions: Y.Y., S.A., and T.F. performed experiments; Y.Y. and S.N. analyzed data; Y.Y. prepared figures; Y.Y. drafted manuscript; Y.Y., S.A., T.F., H.K., Y.S., H.E., M.K., J.R.G., and S.N. approved final version of manuscript; H.K., Y.S., H.E., M.K., J.R.G., and S.N. interpreted results of experiments; J.R.G. and S.N. conception and design of research; J.R.G. and S.N. edited and revised manuscript.

## REFERENCES

1. **[Anon].** Schistosomes, liver flukes, and *Helicobacter pylori*. IARC Working Group on the Evaluation of Carcinogenic Risks to Humans. Lyon, 7–14 June 1994. *IARC Monogr Eval Carcinog Risks Hum* 61: 1–241, 1994.
2. **Goldenring JR, Nomura S.** Differentiation of the gastric mucosa III. Animal models of oxyntic atrophy and metaplasia. *Am J Physiol Gastrointest Liver Physiol* 291: G999–G1004, 2006.
3. **Goldenring JR, Poulsom R, Ray GS, Wright N, Meise KS, Coffey RJ Jr.** Expression of trefoil peptides in the gastric mucosa of transgenic mice overexpressing transforming growth factor-alpha. *Growth Factors* 13: 111–119, 1996.

3a. **Goldenring JR, Ray GS, Coffey RJ, Meunier PC, Haley PJ, Barnes TB, Car BD.** Reversible drug-induced oxyntic atrophy in rats. *Gastroenterology* 118: 1080–1093, 2000.

4. **Halldorsdottir AM, Sigurdardottrir M, Jonasson JG, Oddsdóttir M, Magnússon J, Lee JR, Goldenring JR.** Spasmolytic polypeptide-expressing metaplasia (SPEM) associated with gastric cancer in Iceland. *Dig Dis Sci* 48: 431–441, 2003.
5. **Han SU, Lee JH, Kim WH, Cho YK, Kim MW.** Significant correlation between serum level of hepatocyte growth factor and progression of gastric carcinoma. *World J Surg* 23: 1176–1180, 1999.
6. **Inoue T, Kataoka H, Goto K, Nagaike K, Igami K, Naka D, Kitamura N, Miyazawa K.** Activation of c-Met (hepatocyte growth factor receptor) in human gastric cancer tissue. *Cancer Sci* 95: 803–808, 2004.
7. **Itoh H, Naganuma S, Takeda N, Miyata S, Uchinokura S, Fukushima T, Uchiyama S, Tanaka H, Nagaike K, Shimomura T, Miyazawa K, Yamada G, Kitamura N, Koono M, Kataoka H.** Regeneration of injured intestinal mucosa is impaired in hepatocyte growth factor activator-deficient mice. *Gastroenterology* 127: 1423–435, 2004.
8. **Kataoka H, Miyata S, Uchinokura S, Itoh H.** Roles of hepatocyte growth factor (HGF) activator and HGF activator inhibitor in the pericellular activation of HGF/scatter factor. *Cancer Metastasis Rev* 22: 223–236, 2003.
9. **Konda Y, Kamimura H, Yokota H, Hayashi N, Sugano K, Takeuchi T.** Gastrin stimulates the growth of gastric pit with less-differentiated features. *Am J Physiol Gastrointest Liver Physiol* 277: G773–G784, 1999.
10. **Konturek PC, Kania J, Kukharsky V, Ocker S, Hahn EG, Konturek SJ.** Influence of gastrin on the expression of cyclooxygenase-2, hepatocyte growth factor and apoptosis-related proteins in gastric epithelial cells. *J Physiol Pharmacol* 54: 17–32, 2003.
11. **Miyazawa K, Shimomura T, Naka D, Kitamura N.** Proteolytic activation of hepatocyte growth factor in response to tissue injury. *J Biol Chem* 269: 8966–8970, 1994.
12. **Miyazawa K.** Hepatocyte growth factor activator (HGFA): a serine protease that links tissue injury to activation of hepatocyte growth factor. *FEBS J* 277: 2208–2214, 2010.
13. **Montesano R, Matsumoto K, Nakamura T, Orci L.** Identification of a fibroblast-derived epithelial morphogen as hepatocyte growth factor. *Cell* 67: 901–908, 1991.
14. **Nakamura T, Nawa K, Ichihara A.** Partial purification and characterization of hepatocyte growth factor from serum of hepatectomized rats. *Biochem Biophys Res Commun* 122: 1450–1459, 1984.
15. **Nakamura T, Nishizawa T, Hagiya M, Seki T, Shimonishi M, Sugimura A, Tashiro K, Shimizu S.** Molecular cloning and expression of human hepatocyte growth factor. *Nature* 342: 440–443, 1989.
16. **Nam KT, Lee HJ, Sousa JF, Weis VG, O'Neal RL, Finke PE, Romero-Gallo J, Shi G, Mills JC, Peek RM Jr, Konieczny SF, Goldenring JR.** Mature chief cells are cryptic progenitors for metaplasia in the stomach. *Gastroenterology* 139: 2028–2037, 2010.
17. **Neuburger P, Lewin M, de Recherche C, Bonfils S.** Parietal and chief cell populations in four cases of the Zollinger-Ellison syndrome. *Gastroenterology* 63: 937–942, 1972.
18. **Nomura S, Baxter T, Yamaguchi H, Leys C, Vartapetian AB, Fox JG, Lee3 JR, Wang TC, Goldenring JR.** Spasmolytic polypeptide expressing metaplasia to preneoplasia in *H. felis*-infected mice. *Gastroenterology* 127: 582–594, 2004.
19. **Nomura S, Yamaguchi H, Ogawa M, Wang TC, Lee JR, Goldenring JR.** Alterations in gastric mucosal lineages induced by acute oxyntic atrophy in wild-type and gastrin-deficient mice. *Am J Physiol Gastrointest Liver Physiol* 288: G362–G375, 2005.
20. **Nozaki K, Ogawa M, Williams JA, Lafleur BJ, Ng V, Drapkin RI, Mills JC, Konieczny SF, Nomura S, Goldenring JR.** A molecular signature of gastric metaplasia arising in response to acute parietal cell loss. *Gastroenterology* 134: 511–522, 2008.
21. **Ogawa M, Nomura S, Car BD, Goldenring JR.** Omeprazole treatment ameliorates oxyntic atrophy induced by DMP-777. *Dig Dis Sci* 51: 431–439, 2006.
22. **Ogawa M, Nomura S, Varro A, Wang TC, Goldenring JR.** Altered metaplastic response of waved-2 EGF receptor mutant mice to acute oxyntic atrophy. *Am J Physiol Gastrointest Liver Physiol* 290: G793–G804, 2006.
23. **Parsonnet J, Vandersteen D, Goates J, Sibley RK, Pritikin J, Chang Y.** *Helicobacter pylori* infection in intestinal- and diffuse-type gastric adenocarcinomas. *J Natl Cancer Inst* 83: 640–643, 1991.
25. **Schmidt PH, Lee JR, Joshi V, Playford RJ, Poulsom R, Wright NA, Goldenring JR.** Identification of a metaplastic cell lineage associated with human gastric adenocarcinoma. *Lab Invest* 79: 639–646, 1999.
26. **Stoker M, Gherardi E, Perryman M, Gray J.** Scatter factor is a fibroblast-derived modulator of epithelial cell mobility. *Nature* 327: 239–242, 1987.
27. **Terano A, Hiraishi H, Shimada T, Takahashi M, Yoshiura K, Horie-Sakata K.** Cell culture model for antiulcerogenic agents. *Microsc Res Tech* 53: 389–395, 2001.
28. **Uemura N, Okamoto S, Yamamoto S, Matsumura N, Yamaguchi S, Yamakido M, Taniyama K, Sasaki N, Schlemper RJ.** Helicobacter pylori infection and the development of gastric cancer. *N Engl J Med* 345: 784–789, 2001.
29. **Yamaguchi H, Goldenring JR, Kaminishi M, Lee JR.** Identification of spasmolytic polypeptide expressing metaplasia (SPEM) in remnant gastric cancer and surveillance postgastrectomy biopsies. *Dig Dis Sci* 47: 573–578, 2002.

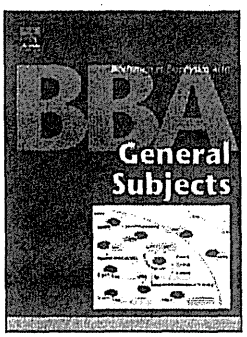


Mitochonrial fumarate reductas as a target of chemotherapy: From patrasites to cancer cells

Chika Sakai, Eriko Tomitsuka, Hiroyasu Esumi, Shigeharu Harada, Kiyoshi Kita

PII: S0304-4165(11)00305-9
DOI: doi: 10.1016/j.bbagen.2011.12.013
Reference: BBAGEN 27149

To appear in: *BBA - General Subjects*

Received date: 27 July 2011
Revised date: 28 November 2011
Accepted date: 17 December 2011

Please cite this article as: Chika Sakai, Eriko Tomitsuka, Hiroyasu Esumi, Shigeharu Harada, Kiyoshi Kita, Mitochonrial fumarate reductas as a target of chemotherapy: From patrasites to cancer cells, *BBA - General Subjects* (2011), doi: 10.1016/j.bbagen.2011.12.013

**Mitochonrial fumarate reductas as a target of chemotherapy:**

**from patrasites to cancer cells**

Chika Sakai[a], Eriko Tomitsuka[a, b], Hiroyasu Esumi[b], Shigeharu Harada[c], Kiyoshi Kita[a,1]

[a]*Department of Biomedical Chemistry, Graduate School of Medicine, The University of Tokyo, Tokyo 113-0033, Japan*

[b] *Cancer Physiology Project, Investigative Treatment Division, National Cancer Center Research Institute East, 6-5-1 Kashiwanoha, Kasiwa, Chiba 277-8577, Japan*

[c]*Department of Applied Biology, Graduate School of Science and Technology, Kyoto Institute of Technology, Kyoto 606-8585, Japan*

[1]To whom correspondence should be addressed: Department of Biomedical Chemistry, Graduate School of Medicine, The University of Tokyo, Hongo, Bunkyo-ku, Tokyo 113-0033, Japan. Tel: +81-3-5841-3526; Fax: +81-3-5841-3444; kitak@m.u-tokyo.ac.jp (Kiyoshi Kita)

Kyewords: mitochondrial fumarate respiration, complex II, hypoxia, drug target, *Ascaris suum*, Type II flavoprotein subunit

Abbreviations: FRD, fumarate reductase; L3, 3rd stage larvae; LL3, lung stage L3; MK, menaquinone; SDH, succinate dehydrogenase; SQR, succinate-ubiquinone reductase; TCA cycle, tricarboxylic acid cycle, QFR, quinol-fumarate reductase; RQ, rhodoquinone

## Abstract

Recent research on respiratory chain of the parasitic helminth, *Ascaris suum* has shown that the mitochondrial NADH-fumarate reductase system (fumarate respiration), which is composed of complex I (NADH-rhodoquinone reductase), rhodoquinone and complex II (rhodoquinol-fumarate reductase) plays an important role in the anaerobic energy metabolism of adult parasites inhabiting hosts. The enzymes in these parasite-specific pathways are potential target for chemotherapy. We isolated a novel compound, nafuredin, from *Aspergillus niger*, which inhibits NADH-fumarate reductase in helminth mitochondria at nM order. It competes for the quinone-binding site in complex I and shows high selective toxicity to the helminth enzyme. Moreover, nafuredin exerts anthelmintic activity against *Haemonchus contortus* in *in vivo* trials with sheep indicating that mitochondrial complex I is a promising target for chemotherapy. In addition to complex I, complex II is a good target because its catalytic direction is reverse of succinate-ubiquionone reductase in the host complex II. Furthermore, we found atpenin and flutolanil strongly and specifically inhibit mitochondrial complex II.

Interestingly, fumarate respiration was found not only in the prasites but also some types of human cancer cells. Analysis of the mitochondria from the cancer cells identified an anti-helminthic as a specific inhibitor of the fumarate respiration. Role of isoforms of human complex II in the hypoxic condition of cancer cells and fetal tissues is a challenge.


## Highlights

Fumarate respiration plays an important role in the anaerobic energy metabolism of parasites.

Fumarate respiration is found not only in the parasites but also some types of human cancer cells.

Fumarate respiration is a good target of chemotherapy for both parasites and cancer.

Important role of human complex II isoforms in the hypoxic condition of cancer cells and fetal tissues

## 1. Introduction

In the general understanding of bioenergetics of higher eukaryotes, oxygen is a most important terminal electron acceptor of mitochondrial respiratory chain (Fig. 1). The major function of the aerobic respiratory chain is the electrogenic translocation of protons out of the mitochondrial or bacterial membrane to generate the proton motive force that drives ATP synthesis by $F_oF_1$-ATPase. This mechanism of oxidative phosphorylation is conserved basically from aerobic bacteria to human mitochondria. However, recent study on the respiratory chain of the lower eukaryotes which reside micro-aerophilic environment has shown that the mitochondrial NADH-fumarate reductase system (fumarate respiration) plays an important role in the anaerobic energy metabolism [1]. This system is composed of complex I (NADH-quinone reductase), low potential quinone species and complex II (quinol-fumarate reductase: QFR).

Fumarate respiration is well known electron transport chain in the anaerobic bacteria [2]. Reducing equivalent of NADH is transferred to low potential quinone such as naphthoquione by complex I and finally is oxidized by fumarate by the fumarate reductase activity of complex II which is a reverse reaction of succinate-ubiquinone reductase (SQR) activity of complex II. By using this respiratory chain, bacteria are able to synthesize ATP even in the absence of oxygen. Recent our study of parasitic nematode, *Ascaris suum*, showed fumarate respiration also plays an important role in the anaerobic energy metabolism of adult worms, which reside in the host small intestine where oxygentension is low [1]. Although fumarate reductase activities of bacterial and mitochondrial complex IIs are the same reaction, evolutional positions of each enzyme are quite different. All four subunits of complex II in adult *A. suum* are more closely related to the bacterial and mitochondrial SQR than to bacterial QFR [3-5]. Thus, mitochondrial QFR is a new enzyme evolved by "reverse evolution" of SQR rather than direct evolution from bacterial QFR [6].

Recent our study has revealed that fumarate respiration functions in some human cancer cells and supports a survival of cancer cells in low nutrition and low oxygen conditions [7, 8]. Furthermore, we found complex II with high QFR activity produces reactive oxygen species (ROS) [9]. ROS has been reported to contribute to proliferation and metastasis of cancer cells via the stabilization of hypoxia-inducible factor-1 (HIF-1) [10]. In addition, succinate produced by fumarate respiration also stabilize HIF-1 by the product inhibition of HIF prolyl hydroxylase, which catalyzes the oxygen-dependent hydroxylation of the conserved proline residues in HIF-1 $\alpha$ [11]. Thus, relationship between accumulation of succinate resulted from functional defect of human complex II by the mutation of the subunits and carcinogenesis has recently become a focus of research [8].

As fumarate respiration is essential for the growth and survival of the parasites and some cancer cells, it should be a promising target of chemotherapy for both parasitic diseases and cancer. In this review, we focus on recent advances in the study of parasite and human mitochondrial fumarate respiration and complex II which is an important component of the system [8].

## 2. Fumarate respiration of parasite mitochondria

### *2.1 Life Cycle of A. suum and Changes in Respiratory Chain*

*A. suum* is the most widely known parasite, and has been studied as a representative of human and livestock parasites [12-14]. Because of its large size, *A. suum* is an ideal for the study including biochemical analysis. Adult *A. suum* resides in the small intestine of mammals, and the female produces between 200,000 and 400,000 fertilized eggs per day (Fig. 2). Eggs are excreted with feces and become mature eggs containing infectious 3rd stage larvae (L3) in about 2-3 weeks at normal temperature. The eggs reach the small intestine and hatch, when orally ingested by a host. A hatched larva invades the intestinal wall, and migrates to the liver, lung, trachea, and pharyngeal region, and finally returns to the intestine via the esophagus and stomach, and becomes an adult worm. In humans, the larvae of *A. suum* migrate to several organs including liver and lung and cause a wide variety of nonspecific symptoms such as general malaise, cough, liver dysfunction, hypereosinophilia with hepatomegaly and/or pneumonia. The oxygen concentration of the small intestine (~5%) is approximately 25 % of that outside the body, and provides an environment of low oxygen tension in which the energy metabolism of the adult differs considerably from that of the larvae and the host (Fig. 3). The phosphoenolpyruvate carboxykinase (PEPCK)-succinate pathway, an anaerobic glycolytic pathway, operates in the adult worm, producing ATP under such a hypoxic conditions. This system is used by many other parasites such as *Echinococcus multilocularis* [15], and has also been observed in the adductor muscle of oysters and other bivalves that require energy conversion under anaerobic conditions. It is therefore considered to be a very common pathway for energy metabolism in adaptation to hypoxic environment [16, 17].

The first half of the PEPCK-succinate pathway is the same glycolytic pathway found in mammals, in which phosphoenolpyruvate (PEP) is produced. In contrast to aerobic metabolism in mammals involving the conversion of PEP to pyruvate by pyruvate kinase, the *A. suum* adult fixes $CO_2$ with PEPCK to produce oxaloacetate (OAA). The OAA is converted to malate by the reverse reaction of malate dehydrogenase and transported into the mitochondria to produce pyruvate and fumarate. The NADH formed during production of pyruvate from malate is used in the reduction of fumarate to succinate. The NADH-fumarate reductase system, which is the anaerobic electron transport system characteristic of adult *A. suum* mitochondria, is the final step of this pathway. Unique property of this pathway is discussed in the next section.

In contrast to larvae which require oxygen for their development and possesses the respiratory system to be almost the same as that of mammals, cytochrome *c* oxidase (Complex IV) is not found in the respiratory chain of adult *A. suum* mitochondria, and the content of ubiquinol-cytochrome *c* reductase complex (Complex III) is extremely low [18]. In addition to the enzymes, quinone species in the mitochondria also change during the life cycle of *A. suum*. In contrast to adult mitochondria, in which the low-potential rhodoquinone (RQ ; $E$m'= -63mV) is the major quinone, ubiquinone (UQ ; $E$m'= +110mV) is the major quinone of larvae (Fig. 4A) [19]. A combination of SQR and UQ,

and that of QFR and a low-potential quinone, such as RQ or menaquinone (MK), is also observed in *E. coli* and other bacteria during metabolic adaptation to changes in oxygen supply [20, 21]. Lower potential of RQ and MK is favorable for the electron transfer from NADH to fumarate (Fig. 4B). In this way, UQ participates in aerobic metabolism in *A. suum* larva, whereas RQ is participates in anaerobic metabolism in adult *A. suum*.

Although studies have shown a clear difference in energy metabolism between larval and adult *A. suum* mitochondria, little is known about changes in the properties of mitochondria during migration of *A. suum* larvae in the host. As described later, examination of the changes in enzymatic characteristics and subunit composition of *A. suum* larval complex II from lung stage L3 (LL3) larvae obtained from rabbits showed that properties of LL3 mitochondria differed from those of L3 and adult mitochondria [22]. Protein chemical analysis revealed that the change in complex II begins with the anchor subunit, and then occurs in the catalytic subunit. Thus, *A. suum* is able to adapt to changes in oxygen concentration in the environment during its life cycle by dynamic change of respiratory chain.

*2.2 NADH-Fumarate reductase system (fumarare respiration) of A. suum adult*

The final step of the PEPCK-succinate pathway, which plays such an important role in the anaerobic energy metabolism of the *A. suum* adult, is catalyzed by the NADH-fumarate reductase system as described in the previous section. This system is also called "fumarate respiration". The low-potential rhodoquinone transfers reducing equivalent of NADH via complex I to complex II, and finally succinate is produced by quinol fumarate reductase (QFR) activity of complex II. The merit of this system is to synthesize ATP using the coupling site of complex I even in the absence of oxygen, although its energy efficiency is low (Fig. 5).

A similar anaerobic respiration system exists in the mitochondria of many other parasites, and has also been found in bacteria. Extensive studies of bacteria, including *Escherichia coli*, have revealed the details of this system [23, 24]. In *E. coli*, there are two types of complex II, and QFR encoded by the *frd* operon is induced under anaerobic conditions. A low molecular weight mediator between complex I and complex II is menaquinone (MK; $E$m'= -80mV), a low-potential naphthoquinone, in the *E. coli* fumarate respiration. In contrast, under aerobic conditions, SQR encoded by *sdh* operon that catalyzes oxidation of succinate is induced [25]. SQR is a dehydrogenase complex in the respiratory system as well as an enzyme in the TCA cycle, and directly connects these systems in aerobic energy metabolism.

Thus, two different enzymes (complex II) are present in *E. coli*, and the bacteria maintain homeostasis of the energy metabolism by controlling synthesis of these enzymes in response to the environmental oxygen supply. How about the complex IIs of *A. suum*? Biochemical and molecular biological analysis showed *A. suum* also possesses two different complex IIs. However, subunit compositions and expression patterns are more complicated in the parasite complex II.

## 3. Complex IIs of *A. suum* mitochondria

### *3.1 Multiple complex IIs in A. suum mitochondria*

The complex II superfamily comprises succinate-quinone reductase (SQR) and quinol-fumarate reductase (QFR), which catalyze the interconversion of succinate and fumarate with quinone and quinol. SQR is a component of the aerobic respiratory chain as well as the tricarboxylic acid (TCA) cycle [26]. QFR is a component of the anaerobic respiratory chain in anaerobic and facultative anaerobic bacteria [27] and lower eukaryotes [6, 28]. SQR and QFR complexes generally consist of four subunits referred to as the flavoprotein subunit (Fp), iron-sulfur subunit (Ip), cytochrome *b* large subunit (CybL), and cytochrome *b* small subunit (CybS). The Fp and Ip subunits comprise the catalytic domain of the enzyme. The Fp subunit has an FAD as a prosthetic group and contains the dicarboxylate-binding site. The Ip subunit generally contains three iron-sulfur clusters $[2Fe\text{-}2S]^{2+,1+}$, $[4Fe\text{-}4S]^{2+,1+}$, and $[3Fe\text{-}4S]^{1+,0}$. Subunits CybL and CybS, with heme *b* as the prosthetic group, form the anchor domain of the enzyme. This anchors the catalytic domain to the inner mitochondrial membrane and also serves as the quinone oxidation/reduction site [29].

Our previous study showed that *A. suum* mitochondria express stage-specific isoforms of complex II (SQR in larvae/QFR in adult) (Fig. 6). The Fp and CybS in adult complex II differ from those of infective third stage larval (L3) complex II. In contrast, there is no difference in the iron-sulfur cluster (Ip) and CybL between adult and L3 isoforms of complex II. However, recent analysis of the changes that occur in the respiratory chain of *A. suum* larvae during their migration in the host, we found that enzymatic activity, quinone content and complex II subunit composition in mitochondria of lung stage L3 (LL3) *A. suum* larvae is different from those of L3 and adult [22]. Quantitative analysis of quinone content in LL3 mitochondria showed that ubiquinone is more abundant than rhodoquinone. Interestingly, the results of two-dimensional bule-native/sodium dodecyl sulfate polyacrylamide gel electrophoresis analyses showed that LL3 mitochondria contained larval Fp ($Fp^{L}$) and adult Fp ($Fp^{A}$) at a ratio of 1 : 0.56, and that most LL3 CybS subunits were of the adult form ($CybS^{A}$). This result clearly indicates that the rearrangement of complex II begins with a change in the isoform of the anchor CybS subunit, followed by a similar change in the Fp subunit. At any event, the NADH-fumarate reductase activity of *A. suum* adult worms (~100 nmol/min/mg) are much higher than that of the mammalian host (2~5 nmol/min/mg).

### *3.2 ROS production from complex II*

Mitochondrial respiratory chain is a significant source of cellular ROS. Impairment of the respiratory chain complexes is known to increase the cellular ROS production [30]. In general, complexes I and III are considered as the two major sites of superoxide and hydrogen peroxide production in the respiratory chain [30-33]. Interestingly, our results show that complex II is the main site of ROS production in *A. suum* adult respiratory chain [9].

Analysis of submitochondrial particles for superoxide ($O_2^{\cdot-}$) production using superoxide dismutase inhibitable acetylated cytochrome *c* reduction, and hydrogen peroxide production using catalase inhibitable amplex red oxidation, in the presence and absence of respiratory chain inhibitors, showed the contribution from both the FAD site and quinone-binding site of complex II to produce $O_2^{\cdot-}$ and $H_2O_2$ when succinate is oxidized under aerobic conditions. Considering the conservation of amino acid residues critical for the enzyme reaction between *A. suum* complex II and mitochondrial SQR, our results show the ROS production from more than one site in mitochondrial complex II linked with subtle differences in the amino acid sequences of the enzyme complex.

*A. suum* adult complex II is a good model to study the mechanism of ROS production from mitochondrial complex II, since amino acid residues conserved among the catalytic domains in mitochondrial SQR enzymes are well conserved in this enzyme and it produces high levels of ROS. Absence of complex III and IV activities in its respiratory chain is an additional advantage of this model. These studies will provide further insight into the possibility of high levels of ROS production from both the FAD site and the Q site in the complex II of *A. suum* adult worm and help to understand the role of mutations in human complex II for carcinogenesis.

*3.3 Specific inhibitors of complex II*

The differences between parasite and host mitochondria described in this review hold great promise as targets for chemotherapy. For example, the anti-malarial drug Atovaquone, which recently developed, acts on the mitochondrial respiratory chain [34]. Atovaquone is effective against chloroquine-resistant strains, [35]. The specific target is thought to be complex III, and biochemical analysis has shown that it acts on the ubiquinone oxidation site in the cytochrome *b* of complex III [36, 37]. Such a chemotherapeutic approach is also applicable to the helminthes. It has been proposed that the fumarate respiration is the target of such drugs as bithionol and thiabendazole [38, 39], but there is no clear biochemical or pharmaceutical evidence to support this idea. However, as described in the previous section, progress in the study of the NADH-fumarate reductase pathway permits screening of new anthelmintic compound. Nafuredin, selectively inhibits helminth complex I at concentrations in the order of nanomoles [40] (Fig. 7). Kinetic analysis revealed that the inhibition by nafuredin is competitive against RQ (Fig. 5). These findings, coupled with the fact that helminth complex I uses both RQ and UQ as an electron acceptor, suggest that the structural features of the quinone reduction site of helminth complex I may differ from that of mammalian complex I. In fact, the inhibitory mechanism of quinazolines, which effectively kill the *E. multilocularis* protoscoleces, was competitive and partially competitive against RQ and UQ, respectively [41].

The most potent inhibitor of complex II, Atpenin A5, was found during the screening of inhibitors for *A. suum* complex II [42]. To our regret, $IC_{50}$ of Atpenin A5 for bovine complex II (3.6 nM) was lower than that for *A. suum* complex II (12 nM for QFR and 32 nM for SQR). However, the further screening of inhibitors showed that flutolanil, a commercially available fungicide, specifically inhibits *A. suum* SQR [43] (Fig 7). The $IC_{50}$ of flutolanil against *A. suum* and bovine SQR was 0.081 and 16 μM, respectively, indicating that

flutolanil is a promising lead compound for anthelminthics. To enable rational drug optimization, a crystal of the *A. suum* QFR complexed with flutolanil was prepared by soaking, and X-ray structure analysis has been performed. The current structural model of the flutolanil bound form of the *A. suum* QFR (Harada, unpublished observation) indicates that flutolanil is bound to the same site as those of the quinone binding observed in complex IIs from pig heart mitochondria (pdb code 1ZOY), *E. coli* (1NEK and 1L0V) and avian (1YQ4). The site of the pig enzyme, for example, is composed of ten residues highly conserved across amino acid sequences of these complex IIs; Pro169, Trp173 and Ile218 from the Ip subunit, Ile30, Trp35, Met39, Ser42, Ile43 and Arg46 from the CybL subunit, and Tyr91 from the CybS subunit. However, three residues, Trp35, Met39 and Ile53, are replaced by Pro65, Trp69 and Gly73, respectively, in *A. suum* QFR. The structures of the *A. suum* QFR together with those of QFRs from *Wolinella succinogenes* [24] and *E. coli* [23], and SQRs from *E. coli* [44], pig heart mitochondria [45], and avian heart mitochondria [46] should help clarify the structure-function relationship of complex II and provide useful information for the structure-based design of anthelminthics.

## 4. Fumarate respiration of human mitochondria

### *4.1 Human complex II*

In human, many cases of diseases caused by mutations in subunits of complex II have been reported. Mutations found in the Ip, Cyb L or Cyb S are associated with the development of pheochromocytoma and paraganglioma [47-51]. The causes of tumorigenesis are suggested that ROS production from mutated complex II [52, 53]or accumulation of succinate as a result of SQR inhibition [11]. Accumulated succinate inhibits HIF-1α prolyl hydroxylases in the cytosol, leading to stabilization and activation of HIF-1α. Thus, succinate can increase expression of genes that facilitate angiogenesis, metastasis, and glycolysis, ultimately leading to tumor progression. On the other hand, no patient about mutation in Fp linked to tumorigenesis has been reported. There are two Fp isoforms in human, which will be discussed later, and this is probably the reason why mutations in Fp are not directly linked to tumorigenesis. Instead, mutations in Fp linked to severe metabolic disorders resulting from decreased activity of the TCA cycle and impairment of oxidative phosphorylation, although these are rare. These autosome-recessive disorders are manifested as childhood encephalopathy, myopathy, adult optic atrophy, and Leigh syndrome [54-57]. Recently, two new proteins, SDHAF1 (succinate dehydrogenase complex assembly factor 1) and SDHAF2, were found to be the first assembly factors of complex II [53, 58]. It was suggested that mutations found in SDHAF1 may result in the reduction of assembled complex II and cause infantile leukoencephalopathy [58]. SDHAF2 is suggested to be required for the incorporation of the flavin adenine dinucleotide cofactor (flavination) of SDHA (succinate dehydrogenase complex, subunit A, flavoprotein), and it is also necessary for complex II assembly and function [53]. Furthermore, the mutation found in SDHAF2 has been suggested to link to familial paraganglioma [53]

*4.2 Isoformes of human complex II*

In 2003, we found two isoforms of human Fp, type I and type II [59, 60] (Fig. 8). These isoforms differ to each other only in two amino acid residues. Tyr 586 and Val 614 of type I Fp are replaced by Phe 586 and Ile 614 in type II Fp, respectively. Tyr 586 and Val 614 are well conserved among mammals' Fps and type II Fp is found only in human complex II (Fig. 9). Type I Fp gene has an exon-intron structure, while the structure of type II Fp gene has not been determined. The type II Fp gene is not found in the NCBI database and the location has not been clarified yet while type I Fp gene is located on chromosome 5p15 [59, 60].

Complex II with type I Fp has isoelectric point (p*I*) of 6 - 7, whereas complex II with type II Fp shows its p*I* of 5 - 6. To explain the difference of p*I* values, several reports suggested the phosphorylation of amino acid residues in Fp subunit [7, 61]. One of these residues, Tyr 500, is located close to Tyr 586, which is replaced by Phe in type II Fp (Fig. 10). Since the Tyr 586 Phe substitution will certainly destroy a hydrogen bond between Tyr 586 $O_\eta$ and Glu 597 $O_\delta$ (3.13Å), the local structure around Tyr 586 as well as Tyr 500 phosphorylation status may be different between Fps of types I and II.

The result of biochemical analysis of complex II with each isoform, complex II with each Fp was found to have almost the same SQR specific activities. However, Type II Fp has lower optimal pH than type I Fp and at optimal pH of type II Fp, $K_m$ value for succinate of type II Fp is lower than type I Fp (Sakai unpublished data). It may be possible that different phosphorylation status of complex II with each isoform cause biochemical differences.

*4.3 Expression of human complex II containing Type II Fp*

Our previous study on the expression of isoformes showed that both types were expressed in all the organs tested (liver, heart, skeletal muscle, brain and kidney) and expression of type I Fp was higher than that of type II Fp [59, 60]. This tendency was also found in the cultured cells such as Fibroblast, Myoblast, Human Umbilical Vein Endothelial Cells (HUV-EC-C), colon cancer cells (HT-29) and lung cancer cells (A549). However, colorectal adenocarcinoma cells (DLD-1), breast cancer cells (MCF-7) and lymphoma cells (Raji) showed higher expression of type II than that of type I Fp. Type I Fp seems to be essential for the ordinary function of complex II because all the examined tissues and many of the cultured cells showed abundant expression of type I Fp and optimum pH for this isoform is around physiological mitochondrial matrix pH (pH8.0).

Since type II Fp was expressed in some cancer cells, this isoform may play an important role in the metabolism of tumor tissue. To investigate the link between type II Fp and tumor tissue in detail, we analyzed mRNA expression ratio of Fp isoforms in several tissues including tumor tissues and cultured cells. Since some tumor marker genes are expressed in fetal tissues, we included the fetal tissues in this analysis.

As shown in Table 1, in cultured cells, all the normal cells tested showed mainly type I Fp expression as reported

previously [59, 60]. In tissues, expression of type I Fp was higher than that of type II Fp in all the organs tested including normal testes tissue. Interestingly, normal pancreatic tissue showed higher expression of type II Fp. In addition, several tumor tissues expressed predominantly type II Fp such as breast tumor, liver tumor, kidney tumor and cervix tumor. Among fetal tissues, brain and skeletal muscle showed higher expression of type II Fp than type I Fp.

*4.4 Fumarate respiration of humen cancer cells*

Several observations suggested the presence of a reverse reaction of complex II, fumarate reductase (FRD), in mammalian cells, although no direct evidence of FRD activity in mammalian complex II has been available until recently [62, 63]. The accumulation of succinate under hypoxic conditions has been reported, and complex II has been suggested to function as FRD in mammalian cells [64]. Metabolome analysis of the cancer cells supports this idea, because succinate, fumarate and malate were present at higher levels in cancer tissues than normal tissues [65]. FRD inhibitor pyrvinium pamoate, an anthelmintic, has also been reported to act as an anticancer compound in human cancer cells [62]. Furthermore, recent biochemical studies showed fumarate respiration in human mitochondria clearly [7, 8 ]. Mitochondria isolated from DLD-1 cells showed FRD activity with 3 nmol/min/mg protein, although this number is quite lower than that of the *A. suum* mitochondria (200 nmol/min/mg). Interestingly, the cancer cells had higher FRD/SQR ratio than the normal cells. For example, FRD/SQR ratio in Panc-1 cells is $0.066 \pm 0.010$, while that in Human Dermal Fibroblast cells is $0.011 \pm 0.002$. In addition, FRD/SQR ratio increased when the cancer cells were cultured under hypoxic and glucose limited condition [7]. Effect of a treatment by phosphatase and protein kinase on the direction of enzyme activity of human complex II suggests the changes from SQR to QFR by phosphorylation of Fp.

Different from *A. suum*, which has at least two distinct complex IIs as mentioned previously, only one gene is found for each subunit of human complex II except Fp. In this connection, it is of interest to speculate that complex II with type II Fp has higher QFR activity and play an important role in fumarate respiration in human mitochondria as terminal oxidase of the system. Further biochemical study on the difference between type I and type II Fp will bring final conclusion on this attractive idea.

**5. Conclusions**

The recent findings described in this review indicate that the respiratory chain plays an important role in responses to changes in the amount of oxygen in the environment. Complex II functions as a fumarate reductase during adaptation to a hypoxic condition to ensure the maintenance of oxygen homeostasis. In this connection, the reports indicating that complex II functions as an oxygen sensor are of great interest [63].

In addition, direct evidences of fumarate respiration in human mitochondria are quite important in the study of

energy metabolism in hypoxic condition including cancer cells. Differences in energy metabolism between hosts and parasites and/or cancer cells are attractive therapeutic targets.

**Acknowledgements**

This work was supported in part by Creative Scientific Research Grant 18GS0314 (to KK), Grant-in-aid for Scientific Research on Priority Areas 18073004 (to KK) from the Japanese Society for the Promotion of Science, and Targeted Proteins Research Program (to KK) from the Japanese Ministry of Education, Science, Culture, Sports and Technology (MEXT).